A microfluidics assisted porous silicon array for optical label-free biochemical sensing

Ilaria Rea,[1] Emanuele Orabona,[1,2] Annalisa Lamberti,[3] Ivo Rendina,[1] and Luca De Stefano[1,a)]
[1]*Institute for Microelectronics and Microsystems - National Council of Research, Naples, Italy*
[2]*Department of Physics, University of Naples "Federico II," Naples, Italy*
[3]*Department of Biochemistry and Medical Biotechnologies, University of Naples "Federico II," Naples, Italy*

(Received 28 April 2011; accepted 28 July 2011; published online 24 August 2011)

A porous silicon (PSi) based microarray has been integrated with a microfluidic system, as a proof of concept device for the optical monitoring of selective label-free DNA-DNA interaction. A 4×4 square matrix of PSi one dimensional photonic crystals, each one of 200 μm diameter and spaced by 600 μm, has been sealed by a polydimethylsiloxane (PDMS) channels circuit. The PSi optical microarray elements have been functionalized by DNA single strands after sealing: the microfluidic circuit allows to reduce significantly the biologicals and chemicals consumption, and also the incubation time with respect to a not integrated device. Theoretical calculations, based on finite element method, taking into account molecular interactions, are in good agreement with the experimental results, and the developed numerical model can be used for device optimization. The functionalization process and the interaction between DNA probe and target has been monitored by spectroscopic reflectometry for each PSi element in the microchannels. © *2011 American Institute of Physics*. [doi:10.1063/1.3626008]

I. INTRODUCTION

The progress in sophisticated micro and nanotechnologies over the last 20 years has led to the development and diffusion of small integrated devices for chemical and biological analyses. Lab on a chip and micro-total-analysis systems are bright examples of what is nowadays more and more required both by industry and academic researches.[1] A subset of these devices are represented by microarrays, originally developed for gene expression profiling:[2] these miniaturized platforms offer the advantages of very high throughput, cost-effective analysis with low consumption of reagents, and quite rapid operative times. Even if DNA microarrays are being rapidly superseded by next generation sequencing technologies in the industrial market, especially in massive parallel sequencing of large numbers of DNA fragments from complex samples or transcriptomes, they are still working-horses devices for small laboratory application in genomics, proteomics, pathogen detection, and also microbial ecology research.[3] From the historical point of view, DNA microarrays were developed utilizing different types of probes, depending on the specific field of investigation, such as oligonucleotides, complementary DNA, long sequences, directly spotted on the support surface, or even growth on it, with a density of sensitive elements from few tenths up to millions of probes. The first generation of microarrays required radioactive or fluorescent labelling, in both cases long, invasive, and costly procedures. To overcome the intrinsic limits of this technology, such as chromophores photobleaching and quenching, label-free optical methods, like surface plasmon resonance imaging, ellipsometry, and microfluidic assisted x-ray diffraction have been proposed.[4–7] In general, DNA microarrays

[a)]Author to whom correspondence should be addressed. Electronic mail: luca.destefano@na.imm.cnr.it. Tel.: +390816132375. Fax: +390816132598.

technology is undergoing significant changes by improving not only the signal detection but also the support materials, the functionalization procedures, the scanning methods, and, last but not least, the integration of microfluidic circuits with the standard devices.

Recently, we have proposed a microarray of porous silicon (Psi) one-dimensional photonic crystals as a functional platform for label-free detection of biomolecular interactions.[8] PSi is by far an attractive support for the immobilization of biological probes due to its sponge-like morphology, constituted by a network of air holes in the silicon matrix, and characterized by a specific surface area of the order of hundreds of square meters per cubic centimetres.[9] PSi can be fabricated by electrochemical etching of doped crystalline silicon in hydrofluoridric acid:[10] since the dissolution process is self-stopping, the content of voids, and thus the dielectric properties, and in particular the refractive index of each silicon layer can be finely tuned by a proper setting of the process parameters. In this way, different mono-dimensional photonic structures, from simple Fabry-Perot interferometer, to complex aperiodic multilayered sequences, showing high quality optical responses, can be obtained by a single-run computer controlled process.[11,12] PSi substrates have been proposed for reverse phase protein and DNA microarray:[13,14] in both applications the nanostructured sensing area with high detection efficiency was the key feature, while the transduction signals were generated by fluorescence and infrared spectroscopy, respectively.

In the present work, we describe the integration of a PSi microarray made of Bragg mirrors with a microfluidic circuit made of polydimethylsiloxane (PDMS): the combination of optics and microfluidics can boost technology towards new devices for biosensing.[15–17] The integration of a PSi transducer in an optical microsystem is never straightforward nor trivial from the technology point of view:[18,19] the applied microfluidic system, which strongly reduces the functionalization time, chemicals and biological products consumption, should also preserve all the features of the PSi label-free optical detection. On the other side, the integration of such optical transducers in a microsystem is an unavoidable step towards the realization of an industrial prototype, which could be considered for production purposes.

II. MATERIALS AND METHODS

A. Microarray fabrication and silanization

The fabrication process of the PSi microarray has been described in details in Ref. 7. Here, we briefly recall main production steps and the integration of the microarray with the microfluidic circuit. A highly doped p^+-type silicon wafer (0.003 Ω cm resistivity, ⟨100⟩ orientation, 400 μm thickness) was used as substrate to realize the microarray. A silicon nitride film, 1.6 μm thick, was deposited on the silicon surface by plasma enhanced chemical vapour deposition. A photolithographic process was used to pattern the silicon nitride film, subsequently etched by reactive ion etching in CHF_3/O_2 atmosphere. The silicon wafer was then electrochemically anodized in a HF-based solution (50 wt. % HF:ethanol = 1:1) in dark and at room temperature. The Bragg reflectors (ten layer pairs) have been realized by alternating high (H) refractive index layers (low porosity) and low (L) refractive index layers (high porosity); a current density of 60 mA/cm^2 was applied for 4 s so as to obtain the high refractive index layers ($n_H = 1.69$) with a porosity of 68% and a thickness of 195 nm, while one of 80 mA/cm^2 was applied for 4 s so as to obtain the low index layers ($n_L = 1.6$) with a porosity of 71% and a thickness of 235 nm (the etch current has been pulsed by steps of 0.2 s followed by 5 s pauses). The layer porosities and thicknesses have been estimated by spectroscopic reflectivity measurements on two single layer samples.[20] Each PSi Bragg reflector was fabricated on the bottom of 12 μm deep microchambers, obtained by applying an electropolishing current density of 800 mA/cm^2 for 30 s. Pore dimension has been increased by rinsing the "as-etched" microarray device in a KOH-ethanol solution (1.5 mM) for 15 min.[21] The device was then oxidized in pure O_2 by a two-step thermal treatment (400 °C for 30 min and 900 °C for 15 min). After the oxidation process, the PSi array was immersed in freshly prepared Piranha solution (H_2SO_4:H_2O_2 = 4:1) for 40 min at room temperature in order to create Si-OH bonds on its surface; the device was then extensively rinsed in deionized water and dried in a stream of nitrogen gas. The Si-OH terminated PSi surface was amino functionalized in a 5% solution of APTES

(3-aminopropyltriethoxysilane) and anhydrous toluene for 30 min at room temperature. After the incubation, the microarray was rinsed twice in anhydrous toluene, dried in nitrogen gas and cured at 100 °C for 10 min.

B. Microfluidic system fabrication

The microfluidic system was designed by a COMPUTER AIDED DESIGN software. The pattern was printed 10 times bigger than its real size on a A4 paper by a laser printer (resolution 1200 dpi) and then transferred on a photographic film (Maco Genius Print Film) by a photographic enlarger (Durst C35) reversely used. As described in Deng *et al.*,[22] the photographic film can be used as photolithographic mask in applications, such as the microfluidics, where high spatial resolution is not required. The designed fluidic system was replicated by photolithographic process on a 10-μm thick negative photoresist (SU-8 2007, MicroChem Corp.) spin-coated for 30 s at 1800 rpm on a silicon substrate. After the photoresist development (SU-8 developer, MicroChem Corp.), the silicon wafer was silanized on exposure to chlorotrimethylsilane (Sigma-Aldrich Co.) vapour for 10 min as anti-sticking treatment. A 10:1 mixture of PDMS prepolymer and curing agent (Sylgard 184, Dow Corning) was prepared and degassed under vacuum for 1 h. The mixture was poured on the patterned wafer and cured on a hot plate at 75 °C for 3 h to facilitate the polymerization and the cross-linking process. After the PDMS layer peeling, inlet and outlet holes were drilled through it in order to allow the access of liquid substances to the system. Finally, the PDMS layer was rinsed in ethanol in a sonic bath for 10 min. The surfaces of PDMS layer and microarray were activated by exposing to oxygen plasma for 10 s to create silanol groups (Si-OH), as shown in the schematic reported in Figure 1(a), aligned under a microscope using an x-y-z theta stage with an accuracy of 5 μm, and sealed together by keeping the two surfaces in contact without any external pressure (Figure 1(b). Figure 1(c) shows a schematic of the PSi array integrated with the microfluidic circuit. The microfluidic device consists of four channels 250 μm wide, 10 μm high, and 3 mm long, each one connecting four PSi elements with a diameter of 200 μm and spaced by 600 μm.

C. Bio-functionalization of the microfluidic PSi array

The PSi microarray elements were bio-functionalized by injecting the solutions into the microfluidic channels using a peristaltic pump (MINIPLUS3, GILSON). Firstly, we have filled the microchannels with a 2.5% glutaraldehyde (GA) solution in 20 mM HEPES buffer (*p*H 7.5) for 30 min; the excess GA was flushed away by 15 μl buffer min^{-1} for 5 min. Then, 5 μl of DNA probe (5′-GGACTTGCCCGAATCTACGTGTCC-3′-NH_2; 200 μM in 10 mM HEPES buffer, *p*H 8) were introduced into each channel and incubated for 3 h at room temperature. The un-attached DNA was removed by flow-through washing with 15 μl buffer min^{-1} for 5 min and with DI water for 2 min. 5 μl of complementary (5′-GGACACGTAGATTCGGGCAAGTCC-3′; 200 μM in 10 mM HEPES buffer, *p*H 7.5) and non-complementary (5′-CACTGTACGTGCGAATTAGGTGAA-3′; 200 μM in 10 mM HEPES buffer, *p*H 7.5) DNA were pumped into two different channels of the

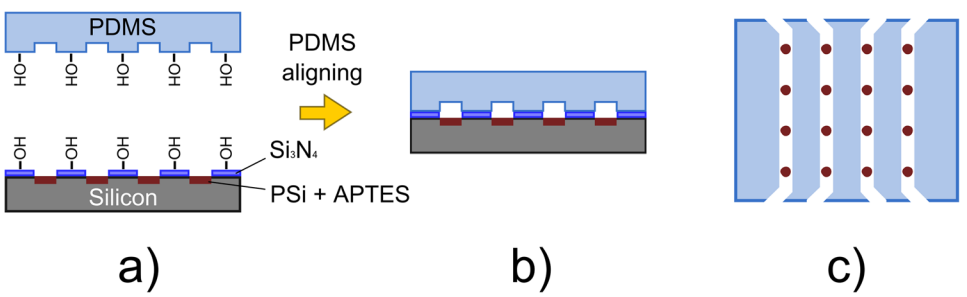

FIG. 1. Schematic illustration of the fabrication process used to integrate the PSi array with a PDMS microfluidic system: (a) plasma activation of the surfaces; (b) sealed device; (c) schematic of the microfluidics.

device and incubated for 1 h. The microchannels have been rinsed in buffer and DI water to remove the excess of biological matter.

D. Microarray optical characterization

The reflectivity spectra of the Bragg reflectors were measured at normal incidence by means of a Y optical reflection probe (Avantes), connected to a white light source and to an optical spectrum analyzer (Ando, AQ6315B). The spectra were collected over the range 600-1000 nm with a resolution of 0.2 nm. The light spot size has been focused on the single PSi device using a $10\times$ microscope objective.

E. Numerical calculations

The finite element package FEMLAB has been used to simulate the bio-functionalization experiment of the PSi elements sealed by the microfluidic circuit. The functionalization dynamic is described by the following differential equations, which represent the interaction between the bioprobes (the DNA) and the active sites (the glutaraldehyde), the Navier-Stokes and the diffusion equations for the fluid motion and the transport of the chemical species in bulk liquid phase, respectively:

$$\frac{\partial B}{\partial t} = k_{on} c \cdot (GA - B) - k_{off} B, \tag{1}$$

$$\frac{\partial \vec{u}}{\partial t} + \vec{u} \cdot \nabla \vec{u} = -\frac{\nabla p}{\rho} + \frac{\mu}{\rho} \nabla^2 \vec{u}, \tag{2}$$

$$\frac{\partial c}{\partial t} + \vec{u} \cdot \nabla c = D_1 \nabla^2 c, \tag{3}$$

where c is the DNA-probe concentration into the channel, k_{on} and k_{off} are the association and dissociation rate constants, GA is the glutaraldehyde surface density on the porous silicon walls, B is the surface density of the bound bioprobes; u, p, ρ, and μ are the velocity field, the pressure, the density (10^3 kg/m^3), and dynamic viscosity (10^{-3} Pa·s) of the fluid, respectively. These equations should be resolved together with the proper boundary and incompressibility conditions, respectively:

$$\vec{n} \cdot (c\vec{u} - D_2 \nabla c) = -\frac{\partial B}{\partial t} (\text{on the reaction surfaces of the PSi elements}) \tag{4}$$

$$\nabla \cdot \vec{u} = 0, \tag{5}$$

D_1 (10^{-11} m^2/s) (Refs. 23 and 24) and D_2 (6.0×10^{-12} m^2/s) are the diffusion coefficients of the chemical specie c in bulk phase and in the PSi pores. Further boundary conditions for the equations are $p = 0$ at the outlet and no-slip walls ($u = 0$) elsewhere. The flow is considered laminar with a parabolic profile at the inlet and an average velocity u_0 (inlet velocity $= 3 \cdot 10^{-3}$ m/s), since the flow in the microchannel is in the low Reynolds number condition.

The interaction equation is usually adopted for antigen-antibody binding, but it can be also used for other biochemical interactions.[23] In the calculations, we have considered only the first few seconds of the bio-functionalization process since the liquid flow rapidly tends to zero and the probes can only diffuse in the available volume. In this approach, the bound probe surface density B can be neglected in the last two terms of Eq. (1). The 3D geometry has been simplified to 2D assuming negligible variations in the concentration across the width of the microchannel. Each PSi element has been modelled as a flat surface on which the D_2 diffusion coefficient of the DNA probe has been supposed constant, since the functionalization process can be considered uniform along the pore walls,[25] and corrected with respect to its value in bulk

solution (D_1) according to the hindered diffusion theory.[26,27] In order to take into account the large specific surface area of the PSi element ($S_{SA} = 100$ m^2/cm^3),[28] we have used in calculations a very high surface density of active sites, *GA*, i.e., the ratio between the glutaraldehyde molecules bound on the PSi element, N_{GA}, and its area, obtained using the equation

$$GA = N_{GA}/A = C_{GA} \bullet d \bullet S_{SA}, \tag{6}$$

where C_{GA} is the density of active sites experimentally measured in a porous silicon layer ($20 \bullet 10^{-5}$ mol/m^2),[29] A is the area of the PSi element ($0.3 \bullet 10^{-3}$ cm^2), and d is its thickness ($4.3 \bullet 10^{-4}$ cm).

III. RESULTS AND DISCUSSION

The images (a) and (b) in Figure 2 show top and lateral views of the microfluidic device compared to a one cent euro coin size (16.25 mm diameter).

The presence of the PDMS layer, which completely seals the array, does not greatly affect the optical spectra of the PSi Bragg reflectors: the reflectivity spectra of a PSi element before and after the sealing process, reported in Figure 3, show a small peak shift of about 3 nm, which is due to humidity condensation. The shift can be removed by a peristaltic pump applied to a close channel, but it rapidly restores when the channel inlet is open. An attenuation of about 30% in the reflected intensity can also be noted, due to the light scattering and absorption in the PDMS layer. The resonance peak wavelength is, on average among all the PSi Bragg, equal to 730 ± 2 nm, the error being the standard deviation.

Moreover, the microfluidic channels greatly facilitate the functionalization process of PSi elements: the biochemical solutions containing the GA, as a cross-linker, and the DNA single strands, as bioprobes, can be directly injected into the microfluidic circuit so that only few microlitres are necessary to fill the microchannel zone (about 15 nl) and the inlet and outlet channels (less than 5 μl). PSi optical transducers are completely covered by the passivation solution just using a smaller volume with respect to more than 30 μl required in the functionalization of not integrated PSi devices:[30,31] in this way, we have greatly reduced the reagents consumption and avoided every manual handling.

The grafting of DNA single strand probes on the PSi surface has been verified by spectroscopic reflectometry: the biological molecules attached to pore walls induce an increasing of

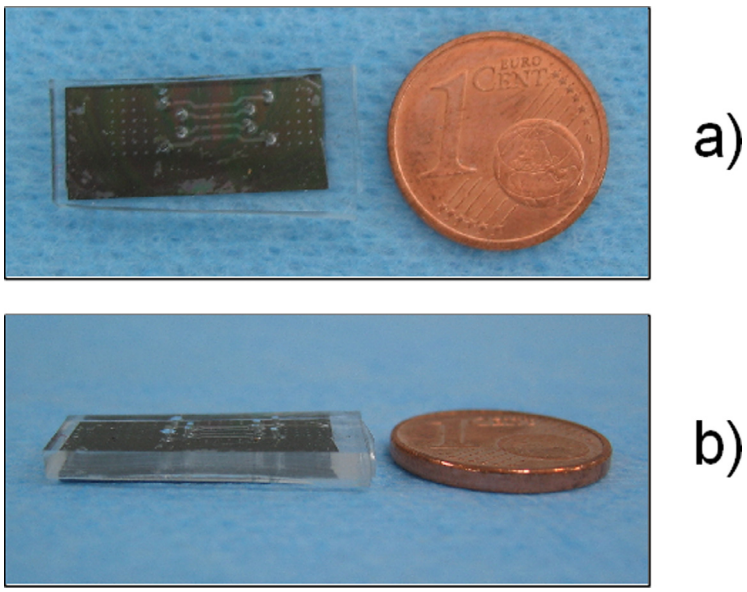

FIG. 2. (a) Top and (b) lateral views of the microfluidic assisted porous silicon array.

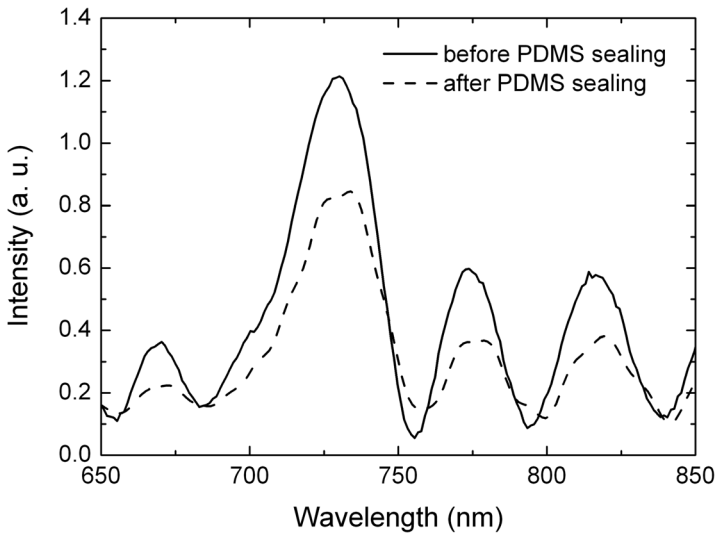

FIG. 3. Reflectivity spectra of a PSi element before (solid line) and after (dashed line) the sealing with the PDMS microfluidic system.

the effective refractive index of the layers and, as consequence, a red-shift of the reflectivity spectrum of each PSi optical transducers.

In Figure 4, we reported the spectra of four PSi Bragg reflectors, belonging to the same microchannel, before and after the DNA functionalization process: an average red-shift of 18 ± 2 nm has been measured, which is a value higher than 10.4 ± 0.6 nm obtained in the case of a not integrated PSi microarray.[7] The red-shift increase observed in the integrated device is simply due to a higher ratio [GA active sites available/DNA probe concentration], with respect

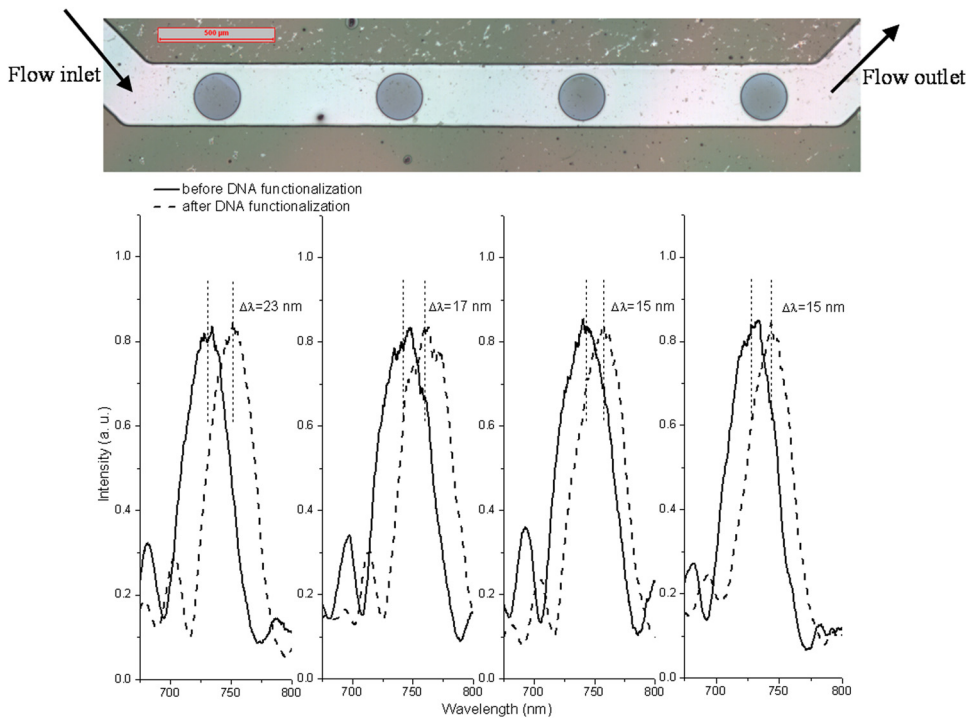

FIG. 4. Top image: optical micrograph of a microfluidic channel. Bottom image: reflectivity spectra of the PSi elements before (solid line) and after (dashed line) the DNA probe functionalization.

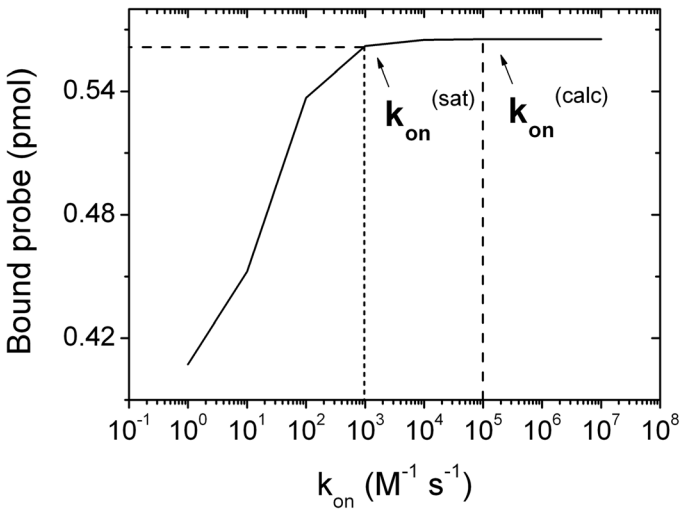

FIG. 5. DNA probes bound to the porous silicon surface calculated for different values of the association rate, k_{on}.

to the case of the array without microfluidics. We have also observed a significant shortening of the process time: we incubated the bioprobes for only 3 h instead of the overnight treatment reserved to free PSi samples. The reduction of the incubation time can be justified by considering the diffusion of the DNA molecules in a solution according to the Fick's law;[32] the diffusion time of a DNA single strand (25 mer, 7.7 kDa), characterized by a diffusion coefficient of about 10^{-11} m^2/s at room temperature,[24] is, in fact, three orders of magnitude lower in a nanolitre volume with respect to a microlitre one. Anyway, the microfluidic circuit, we have fabricated cannot be simply schematized as a small volume; for this reason, we have experimentally determined, which was the incubation time to be used by measuring the red-shifts of the optical spectra after 2, 3, 4, and 8 h. The 3 h incubation was chosen, since we found that the red-shift after 4 h was equal to that obtained after 3 h and greater than that measured after 2 h. The sample incubated for 8 h shown a red-shift less than the 2 h sample, which means that the PSi matrix was partially dissolved by the buffer.

The red-shift due to DNA functionalization is not equal for all the Bragg spectra: its magnitude decreases from 23 nm to 15 nm along the flow propagation direction. The phenomenon can be due to the decreasing of the DNA probes concentration in the propagation flow caused by the interaction with the GA into the channel.

In order to better understand how the functionalization process proceeds in the microchannels, we have performed numerical calculations. In Eq. (1), we have assumed an association constant $k_{on} = 10^5\ M^{-1} \cdot s^{-1} = k_{on}^{(calc)}$,[23] and we have verified that there are no changes in the amount of DNA probes bound to the PSi surface on increasing or decreasing the association rate value of some magnitude orders, as it can be deduced from the graph reported in Figure 5. In particular, from this graph, it is possible to estimate the association rate value ($k_{on}^{(sat)}$), which corresponds to the saturation of the binding sites available. $k_{on}^{(sat)}$ is two orders of magnitude lower with respect to that used in our calculations.

In Figure 6, the maps of DNA probes concentration available in the first (a) and last (b) microchambers are reported together with the respective mean concentration variations along the length and the depth of the channel. The distribution of DNA probes in the microchamber has been obtained by numerically solving the set of Eqs. (1)–(5) with constants values reported in Sec. 2.5, in particular, the inlet velocity was $u_0 = 3 \cdot 10^{-3}$ m/s. We can clearly observe an inhomogeneous distribution of DNA probes, which we attributed to the starting concentration gradient of the probes, that is, strictly related to the inlet velocity.

We have investigated by numerical simulation how to reduce this effect, and we have found, that by increasing the inlet velocity up to $3 \cdot 10^{-2}$ m/s, the probes concentration becomes uniform along the fluidic channel: the difference between DNA probe concentrations bound on

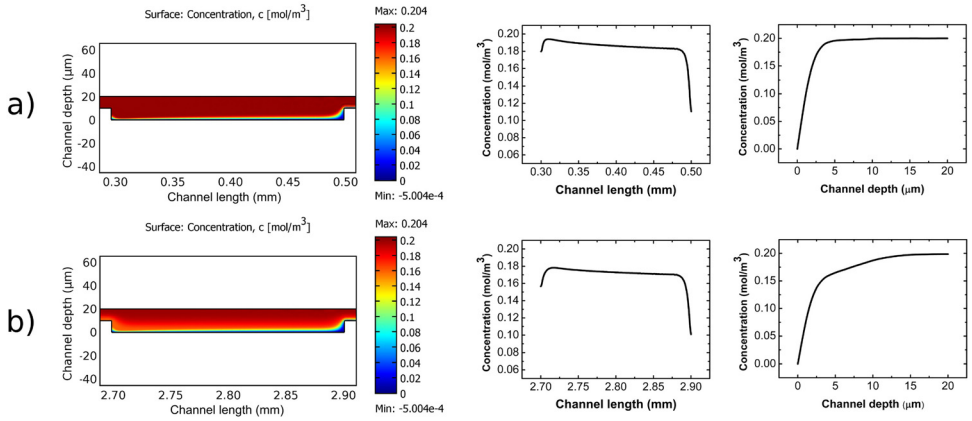

FIG. 6. Comparison between the DNA concentration distribution in the first (a) and last (b) microchambers just after the injection of the probe. A significant difference in DNA probes concentration is well evident. The numerical simulation has been obtained with an inlet velocity of $3 \bullet 10^{-3}$ m/s.

the surfaces of the first and last PSi devices is about 5%. The results of the calculations are illustrated in Figure 7. Even if higher inlet velocity values could damage the device because they correspond to high pressure values by the Hagen-Poiseuille law, we have tested circuit integrity up to $u_0 = 5.4 \bullet 10^{-1}$ m/s. Bio-functionalization experiments repeated by using values equal or greater than $3 \bullet 10^{-2}$ m/s produced peaks shift of all PSi elements, which differ less than 8% among them.

Even if we cannot exclude completely the DNA absorption by channel walls, we believe that in our experiment the surface interaction does not affect the DNA concentration for at least two reasons: PDMS is able to effectively adsorb only small hydrophobic molecules, of the order of hundreds of Daltons,[33] while the DNA probe we used has a molecular weight of 7.7 kDa; moreover, DNA is a highly charged hydrophilic molecule with a reduced spontaneous ability to interact with hydrophobic surfaces.[34]

After the bio-functionalization with DNA probe, we have studied the DNA-DNA hybridization by injecting into the microchannel 200 μM of complementary sequence. Figure 8 shows the reflectivity spectra of a PSi Bragg reflector before the functionalization process, after the DNA functionalization, and after the complementary DNA interaction.

A red-shift of 6.0 ± 0.2 nm can been detected after the specific DNA-DNA interaction by the first PSi element, while an average red-shift of 5 ± 1 nm has been recorded by the other

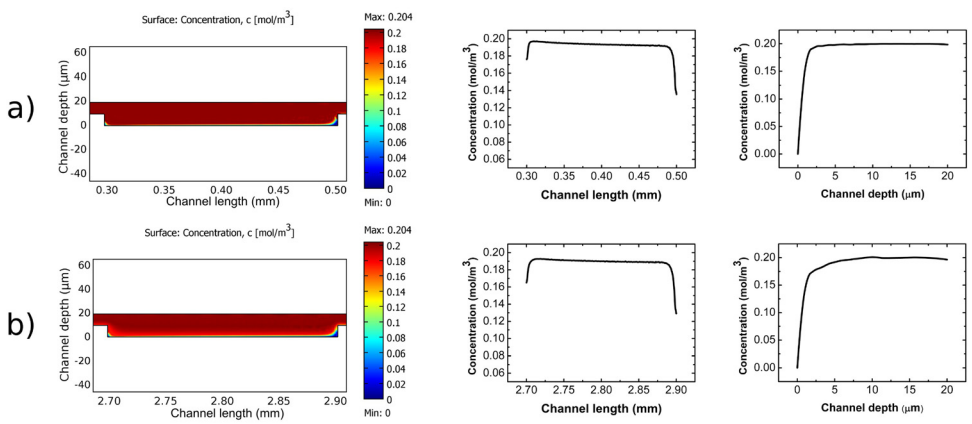

FIG. 7. Maps of DNA concentration distribution in the first (a) and last (b) microchambers together with the mean concentration variations versus the length and the depth of the channel. The data have been calculated using an inlet velocity of $3 \bullet 10^{-2}$ m/s.

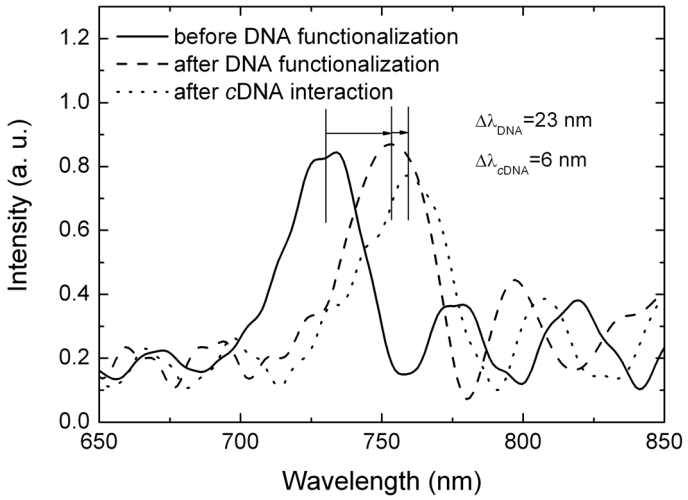

FIG. 8. Reflectivity spectra of a PSi element before (solid line) and after (dashed line) the DNA probe attachment, and after (dotted line) the hybridization with the complementary DNA.

three. A negligible shift, less than 0.2 nm (data not reported in the figure), is the result of a control measurement, which has been done exposing another functionalized microchannel to non-complementary DNA, demonstrating that the integrated PSi array is able to discriminate between complementary and non-complementary interactions. In a previous work, we have experimentally estimated the sensitivity of an optical PSi based DNA hybridization sensor obtaining the value 1.1 nm/μM, which corresponds to a limit of detection of few nM hundreds, in case of a 0.2 nm resolution on the wavelength shift.[31] This value is of the same order of those reported for other DNA biosensors realized using different technologies.[35,36]

A low variability among results of DNA-DNA recognition experiments is a key issue for microarrays application in immunoassays diagnostic or proteomics, so that we have followed the DNA hybridization by two other microfluidic PSi arrays, both realized using the same fabrication process previously reported, obtaining results comparable with those shown in Figure 8. In particular, by averaging over these results, a standard deviation of 4 nm has been estimated for the spectrum red-shift due to the DNA functionalization, while a standard deviation of 1 nm has been calculated for the red-shift related to the DNA-*c*DNA interaction.

IV. CONCLUSIONS

A PSi based microarray integrated with microfluidic microchannels in PDMS for the study of DNA-DNA interactions has been fabricated as a proof of concept device. The PSi elements constituting the array have been functionalized by directly injecting the DNA probe molecules into the microfluidic system. Smaller sample amounts and a functionalization time significantly shorter than those required for the not integrated device have been used. The DNA hybridization has been detected by using a label-free method based on spectroscopic reflectometry. We plan to use the same optical microsystem and numerical method of analysis to design and perform continuous flow experiments in order to avoid difficulties due to static operations. The integrated microarray using a label-free detection method has revealed great potentiality and it could be of interest also in other application fields of the bio-analysis.

[1]D. Mark, S. Haeberle, G. Roth, F. Stettenzab, and R. Zengerlez, Chem. Soc. Rev. **39**, 1153 (2010).
[2]C. Fournier-Wirth and J. Coste, Biologicals **38**, 9 (2010).
[3]S. W. Roh, G. C. J. Abell, K.-H. Kim, Y.-D. Nam, and J.-W. Bae, Trends Biotechnol. **28**, 291 (2010).
[4]M. Bally, M. Halter, J. Janos Voros, and H. M. Grandin, Surf. Interface Anal. **38**, 1442 (2006).
[5]G. Rong, A. Najmaie, J. E. Sipe, and S. M. Weiss, Biosens. Bioelectron. **23**, 1572 (2008).
[6]G. Rong, J. D. Ryckman, R. L. Mernaugh, and S. M. Weiss, Appl. Phys. Lett. **93**, 161109 (2008).
[7]R. Dootz, A. C. Toma, and T. Pfohl, Biomicrofluidics **5**, 024104 (2011).

[8]I. Rea, A. Lamberti, I. Rendina, G. Coppola, M. Gioffrè, M. Iodice, M. Casalino, E. De Tommasi, and L. De Stefano, J. Appl. Phys. **107**, 014513 (2010).
[9]R. Herino, G. Bomchil, K. Barla, C. Bertrand, and J. L. Ginoux, J. Electrochem. Soc. **134**, 1994 (1987).
[10]L. T. Canham, Adv. Mater. **7**, 1033 (1995).
[11]V. Mulloni and L. Pavesi, Appl. Phys. Lett. **76**, 2523 (2000).
[12]L. Moretti, I. Rea, L. Rotiroti, I. Rendina, G. Abbate, A. Marino, and L. De Stefano, Opt. Express **14**, 6264 (2006).
[13]A. Ressine, I. Corin, K. Järås, G. Guanti, C. Simone, G. Marko-Varga, and T. Laurell, Electrophoresis **28**, 4407 (2007).
[14]R. Yamaguchi, K. Miyamoto, K. Ishibashi, A. Hirano, S. M. Said, Y. Kimura, and M. Niwano, J. Appl. Phys. **102**, 014303 (2007).
[15]K. Chin, A. Q. Liu, C. S. Lim, C. L. Lin, T. C. Ayi, and P. H. Yap, Biomicrofluidics 4, 024107 (2010).
[16]Y. Chen, L. Lei, K. Zhang, J. Shi, L. Wang, H. Li, X. M. Zhang, Y. Wang, and H. L. W. Chan, Biomicrofluidics **4**, 043002 (2010).
[17]A. Q. Jian, X. M. Zhang, W. M. Zhu, and M. Yu, Biomicrofluidics **4**, 043008 (2010).
[18]L. De Stefano, K. Malecki, F. G. Della Corte, L. Moretti, I. Rea, L. Rotiroti, and I. Rendina, Sensors **6**, 680 (2006).
[19]L. De Stefano, I. Rea, L. Moretti, F. G. Della Corte, L. Rotiroti, D. Alfieri, and I. Rendina, Phys. Status Solidi A **204**(5), 1459 (2007).
[20]C. Pickering, M. I. J. Beale, D. J. Robbins, P. J. Pearson, and R. Greef, J. Phys. C **17**, 6535 (1984).
[21]L. A. DeLouise and B. L. Miller, Anal. Chem. **76**, 6915 (2004).
[22]T. Deng, H. Wu, S. T. Brittain, and G. M. Whitesides, Anal. Chem. **72**, 3176 (2000).
[23]G. Q. Hu, Y. L. Gao, and D. Q. Li, Biosens. Bioelectron. **22**, 1403 (2007).
[24]R. M. Robertson, S. Laib, and D. E. Smith, PNAS **103**, 7310 (2006).
[25]H. Ouyang, C. C. Striemer, and P. M. Fauchet, Appl. Phys. Lett. **88**, 163108 (2006).
[26]R. E. Beck and J. S. Schultz, Science **170**, 1302 (1970).
[27]J. Shao and R. E. Baltus, AIChE J. **46**, 1149 (2000).
[28]J. Salonen and V.-P. Lehto, Chem. Eng. J. **137**, 162 (2008).
[29]N. H. Voelcker, I. Alfonso, and M. R. Ghadiri, ChemBioChem **9**, 1776 (2008).
[30]L. De Stefano, L. Rotiroti, I. Rea, I. Rendina, P. Arcari, A. Lamberti, and C. Sanges, Sensors **7**, 214 (2007).
[31]E. De Tommasi, I. Rendina, I. Rea, V. Di Sarno, L. Rotiroti, P. Arcari, A. Lamberti, C. Sanges, and L. De Stefano, Sensors **8**, 6549 (2008).
[32]*Cell Physiology Sourcebook: A Molecular Approach*, 3rd ed., edited by N. Sperelakis (Academic, San Diego, 2001).
[33]M. W. Toepke and D. J. Beebe, Lab Chip **6**, 1484 (2006).
[34]C. Wittmann and S. Alegret, *Immobilisation of DNA on Chips* (Springer Science & Business, Berlin, Heidelberg, New York, 2005).
[35]T. M. A. Gronewold, A. Baumgartner, E. Quandt, and M. Famulak, Anal. Chem. **78**, 4865 (2006).
[36]Y. Uludag, X. Li, H. Coleman, S. Efstathiou, and M. A. Cooper, Analyst **133**, 52 (2008).